Use of *ab Initio* Quantum Molecular Similarities as an Interpretative Tool for the Study of Chemical Reactions

Miquel Solà, Jordi Mestres, Ramon Carbó,* and Miquel Duran*

Contribution from the Institut de Química Computacional and Departament de Química, Universitat de Girona, Plaça de l'Hospital 6, 17071 Girona, Catalonia, Spain

*Received October 4, 1993. Revised Manuscript Received March 29, 1994**

Abstract: Quantum molecular similarity measures are used together with structural proximity and isosynchronicity parameters as interpretative tools to understand better how a reaction proceeds along the reaction coordinate. Both Hammond and anti-Hammond behavior can be easily predicted and interpreted by means of the analysis presented. Further, this methodology shows that the effect of a uniform electric field on the reaction coordinate of a Walden inversion reaction should be regarded from the transition state point of view, in such a way that one can say that the reactant complex is becoming transition state-like.

Introduction

(A) Outline of the Problem. The study of organic reactions has experienced a revolution in the last years. The current availability of standard quantum chemistry programs for *ab initio*, density functional, and semiempirical calculations with analytic gradient and vibrational frequency capabilities has given rise to the so-called gradient revolution, which provides a powerful tool for investigating molecular structure and chemical reactivity problems.

However, equally important is the existence of interpretative tools for the analysis of molecular wave functions obtained from any computational source. Mulliken atomic charges,[1] Bader topological analyses,[2] bond orders,[3] natural population analysis,[4] projection of molecular orbital wave functions onto a set of valence-bond structures,[5] Morokuma energy decomposition,[6] and perturbation molecular orbital analysis[7] are, among others, commonly used techniques that, making use of the wave function, allow chemists to gain more insight into the nature of matter and its transformations.

Lately, use of quantum molecular similarity measures (QMSM)[8-17] has become more widespread as an interpretative tool when comparing wave functions of different systems. Similarity measures are especially appropriate when one tries to rationalize reactivity theories based on empirical structure–reactivity relationships (*e.g.*, linear free energy relationships)[18] or to predict the physical properties of a molecule from its molecular structure.

(B) Molecular Similarity. Three-dimensional molecular shape[8] and graph theory[9] have been used to quantify molecular similarity, although the most widely used definition was reported initially by Carbó *et al.*[14] and was based on the assumption that similar molecules must have similar electron distributions. These authors proposed that if the molecules under comparison, A and B, have electron densities D_A and D_B, respectively, then their similarity is given by the expression:[15]

$$Z_{A,B}(\Theta) = \int\int D_A(r_1)\Theta(r_1,r_2)D_B(r_2)\,dr_1\,dr_2 \qquad (1)$$

where $\Theta(r_1,r_2)$ is a positive definite operator depending on two-

* Abstract published in *Advance ACS Abstracts,* May 15, 1994.

(1) Mulliken, R. S. *J. Chem. Phys.* **1955**, *23*, 1833.

(2) Bader, R. F. W. *Acc. Chem. Res.* **1985**, *18*, 9. Bader, R. F. W.; Nguyen-Dang, T. T. *Adv. Quantum Chem.* **1981**, *14*, 63. Bader, R. F. W.; Nguyen-Dang, T. T.; Tal, Y. *Rep. Prog. Phys.* **1981**, *44*, 893.

(3) Pauling, L. *J. Am. Chem. Soc.* **1947**, *69*, 542. Mayer, I. *Int. J. Quantum Chem.* **1986**, *24*, 477. Mayer, I. *Chem. Phys. Lett.* **1983**, *97*, 270. Wiberg, K. A. *Tetrahedron* **1968**, *24*, 1083. Armstrong, D. P.; Perkins, P. G.; Stewart, J. J. P. *J. Chem. Soc., Dalton Trans.* **1973**, 838. Zhan, C. G. *J. Mol. Struct. (Theochem)* **1993**, *101*, 193.

(4) Reed, A. E.; Curtiss, L. A.; Weinhold, F. *Chem. Rev.* **1988**, *88*, 899. Foster, J. P.; Weinhold, F. *J. Am. Chem. Soc.* **1980**, *102*, 7211, Reed, A. E.; Weinhold, F. *J. Chem. Phys.* **1985**, *83*, 1736. Reed, A. E.; Weinstock, R. B.; Weinhold, F. *J. Chem. Phys.* **1985**, *83*, 735.

(5) Hiberty, P. C.; Leforestier, P. C. *J. Am. Chem. Soc.* **1978**, *100*, 2012. Hiberty, P. C.; Ohanessian, G. *J. Am. Chem. Soc.* **1982**, *104*, 66. Hiberty, P. C. *Int. J. Quantum Chem.* **1981**, *19*, 259.

(6) Morokuma, K.; Nagase, S. *J. Am. Chem. Soc.* **1978**, *100*, 1666. Morokuma, K. *Acc. Chem. Res.* **1977**, 294. Umeyama, H.; Kitaura, K.; Morokuma, K. *Chem. Phys. Lett.* **1975**, *36*, 11.

(7) Bernardi, F.; Bottoni, A. In *Computational Theoretical Chemistry*; Csizmadia, I. G., Daudel, R., Eds.; D. Reidel Publishing Co.: Menton, 1980; p 197. Whangbo, M.-H. In *Computational Theoretical Chemistry*; Csizmadia, I. G., Daudel, R., Eds.; D. Reidel Publishing Co.: Menton, 1980; p 233.

(8) Mezey, P. G. *Shape in Chemistry: An Introduction to molecular shape and topology*; VCH Publishers: New York, 1993. Mezey, P. G. In *Concepts and Applications of Molecular Similarity*; Johnson, M. A., Maggiora, G. M., Eds.; Wiley: New York, 1990; p 321. Mezey, P. G. *J. Chem. Inf. Comput. Sci.* **1992**, *32*, 650. Mezey, P. G. In *The Role of Computational Models and Theories in Biotechnology*; Bertrán, J., Ed.; Kluwer Academic Publishers: Dordrecht, 1992; p 83. Mezey, P. G. *J. Math. Chem.* **1992**, *11*, 27. Mezey, P. G. *J. Comput. Chem.* **1987**, *8*, 462.

(9) Grindley, H. M.; Artymiuk, P. J.; Rice, D. W.; Willett, P. *J. Mol. Biol.* **1993**, *229*, 707. Randić, M. *J. Chem. Educ.* **1992**, *69*, 713. Trinajstić, N. *Chemical Graph Theory*; CRC Press: Boca Raton, FL, 1993. Mihalić, Z.; Trinajstić, N. *J. Chem. Educ.* **1992**, *69*, 701. Randić, M. *J. Math. Chem.* **1991**, *7*, 155.

(10) Cioslowski, J.; Fleischmann, E. D. *J. Am. Chem. Soc.* **1991**, *113*, 64.

(11) Cioslowski, J.; Challacombe, M. *Int. J. Quantum Chem. Quantum Chem. Symp.* **1991**, *25*, 81. Ortiz, J. V.; Cioslowski, J. *Chem. Phys. Lett.* **1991**, *185*, 270. Cioslowski, J. *Theor. Chim. Acta* **1992**, *81*, 319.

(12) Cioslowski, J. *J. Am. Chem. Soc.* **1991**, *113*, 6756.

(13) Richard, A. M. *J. Comput. Chem.* **1991**, *12*, 959. Good, A. C.; Hodgkin, E. E.; Richards, W. G. *J. Chem. Inf. Comput. Sci.* **1992**, *32*, 188. Hodgkin, E. E.; Richards, W. G. *Int. J. Quantum Chem. Biol. Symp.* **1987**, *14*, 105. Burt, C.; Huxley, P.; Richards, W. G. *J. Comput. Chem.* **1990**, *11*, 1139. Manaut, F.; Sanz, F.; Jose, J.; Milesi, M. *J. Comput.-Aided Mol. Des.* **1991**, *5*, 371. Sanz, F.; Manaut, F.; Sánchez, J. A.; Loyola, E. *J. Mol. Struct. (Theochem)* **1991**, *230*, 437. Sanz, F.; Manaut, F.; Dot, T.; López de Briñas, E. *J. Mol. Struct. (Theochem)* **1992**, *256*, 287.

(14) Carbó, R.; Arnau, M.; Leyda, L. *Int. J. Quantum Chem.* **1980**, *17*, 1185.

(15) Carbó, R.; Calabuig, B. *Int. J. Quantum Chem.* **1992**, *42*, 1681. Carbó, R.; Besalú, E. In *Proceedings of the First Girona Seminar on Molecular Similarity*; Carbó, R., Ed., in press.

(16) Carbó, R.; Calabuig, B. *Comput. Phys. Commun.* **1989**, *55*, 117. Carbó, R.; Calabuig, B. *J. Mol. Struct. (Theochem)* **1992**, *254*, 517. Carbó, R.; Calabuig, B. *Int. J. Quantum Chem.* **1992**, *42*, 1695. Carbó, R.; Domingo, Ll. *Int. J. Quantum Chem.* **1987**, *32*, 517.

(17) Ponec, R.; Strnad, M. *Collect. Czech. Chem. Commun.* **1987**, *52*, 555. Ponec, R.; Strnad, M. *J. Phys. Org. Chem.* **1991**, *4*, 701. Ponec, R.; Strnad, M. *J. Phys. Org. Chem.* **1992**, *5*, 764. Ponec, R.; Strnad, M. *Int. J. Quantum Chem.* **1992**, *42*, 501.

(18) Brønsted, J. N. *Chem. Rev.* **1928**, *15*, 231. Brønsted, J. N.; Pedersen, K. J. *Z. Phys. Chem.* **1924**, *108*, 185; Bell, R. P. In *Correlation Analysis in Chemistry. Recent Advances*; Chapman, N. B., Shorter, J., Eds.; Plenum Press: New York, 1978; Chapter 2. Hammett, L. P. *Physical Organic Chemistry*; McGraw-Hill: New York, 1970. Marcus, R. A. *Annu. Rev. Phys. Chem.* **1964**, *15*, 155. Marcus, R. A. *J. Phys. Chem.* **1968**, *72*, 891. Cohen, A. D.; Marcus, R. A. *J. Phys. Chem.* **1968**, *72*, 14249. Taft, R. W., Jr. In *Steric Effects in Organic Chemistry*; Newman, M. S., Ed.; Wiley: New York, 1956.

0002-7863/94/1516-5909$04.50/0

electron coordinates. In the particular case that $\Theta(r_1,r_2)$ is the Dirac delta function $\delta(r_1 - r_2)$, the substitution of this function into eq 1 gives the formula for calculating the overlap-like similarity, given that the expression is reduced to a simple overlap integral between densities. Likewise, when $\Theta(r_1,r_2)$ is substituted by $1/r_{12}$ in eq 1, the expression for computing Coulomb-like similarities is obtained, this name coming from the parallelism between this kind of integrals and the so-called Coulomb integrals. Other operators can be used depending on the information one wants to obtain. A more general expression[15] involves first-order density matrices,

$$Z_{A,B}(\Theta) = \int\int D_A(r_1,r_2)\Theta(r_1,r_2)D_B(r_1,r_2)\,dr_1\,dr_2 \quad (2)$$

or even n-order density matrices and multielectron Θ operators.

Finally, once the similarity measure has been defined, a similarity index (I)[14] can be calculated as a generalized cosine of the angle between functions D_A and D_B in eq 1:

$$I_{A,B} = Z_{A,B}(Z_{A,A}Z_{B,B})^{-1/2} \quad (3)$$

This cosine-like index has, for any pair of compared systems, a value between 0 (total dissimilarity) and 1 (complete similarity or identity), depending on the similarity associated with the two molecules.

(C) Hammond Postulate. The Hammond postulate[19] basically states that if the transition state is near in the potential energy surface to an adjacent stable complex, then it is also near in structure to the same complex. This is generally true also when slopes and matrices of force constants associated with reactants and products are similar.[20,21] This postulate, which can be applied to most chemical reactions, has been used for predicting the effects of substituent changes and external perturbations on transition-state geometry.[22] Different methodologies have been developed in trying to rationalize this postulate,[23] most of them based on semiquantitative assumptions. Arteca and Mezey,[21] using energy differences and the first and second derivatives of reactants, products, and transition state, formulated several conditions for the validity of the Hammond postulate on one-dimensional reaction barriers. However, the unique attempt to quantify the Hammond postulate within a quantum mechanical framework is due to Cioslowski.[12] He has shown that the quantification of the Hammond postulate can be achieved by defining two new parameters, the so-called structural proximity of the transition state to the reactants (β) and the isosynchronicity (α) parameters between transition state and stable complexes. These α and β definitions hold for any expression for the distance between A and B ($d_{A,B}$) which satisfies the classical properties of an Euclidean distance. In particular, β is given by

$$\beta = [d_{A,TS} - d_{B,TS}]/d_{A,B} \quad (4)$$

therefore taking values from −1 to 1. If the reactants (A) and transition state (TS) are closer on the potential energy surface than the products (B) and the TS, the β value is negative, and otherwise it is positive. So, a negative value of β corresponds to a reaction with an "early" TS and a positive value to a reaction with a "late" TS.

Furthermore, Cioslowski defined α as

$$\alpha = [d_{A,TS} + d_{B,TS}]/d_{A,B} \quad (5)$$

This parameter is never smaller than 1, and it takes a value near to 1 when the distance from either A or B to the TS is small or in the case of reactions in which the transition state loses its similarity to the reactants in exactly the same way as it gains its similarity to the products.

In the present work, the distance between the molecular electronic distributions of A and B has been taken as:[14]

$$d_{A,B} = [Z_{A,A} + Z_{B,B} - 2Z_{A,B}]^{1/2} \quad (6)$$

Since the value of the distance given by eq 6 depends on the relative spatial orientation of molecules A and B, their mutual orientation is optimized in order to maximize their QMSM, which is equivalent to minimizing the $d_{A,B}$ values used in the evaluation of α and β parameters.

The aim of this paper is to make use of the α and β parameters defined by Cioslowski[12] together with the QMSM and distance defined by Carbó *et al.*[14,15] as an interpretative tool to understand better how a series of reactions proceed along the reaction coordinate and to analyze the changes undergone by the molecular systems when going from reactants to products. This methodology is applied to the study of simple chemical rearrangement reactions with both Hammond and anti-Hammond behavior and also to the analysis of external perturbations on the reaction coordinate of a Walden inversion reaction.

Methodology

The full explanation of the methodology used in this work has been previously reported.[24,25] Basically, an approximate density ($\rho(r)$) is least-squares fitted to the exact charge density ($D(r)$) by minimizing the integral

$$\Delta(\Theta) = \int (D(r_1) - \rho(r_1))\Theta(r_1,r_2)(D(r_2) - \rho(r_2))\,dr_1\,dr_2 \quad (7)$$

subject to the following constraint, necessary to guarantee charge conservation,

$$\int \rho(r)\,dr = N_e \quad (8)$$

N_e being the total number of electrons and $\rho(r)$ being expanded in a set of Gaussian functions as

$$D_1(r) \simeq \rho_1(r) = \sum_{i\in I}^{N_{func}} a_i g_i(r) \quad (9)$$

Use of this fitted density instead of the exact density in eq 1 eliminates the need to evaluate costly four-centered integrals. As a matter of fact, if N_{func} is taken as the number of Gaussian functions used in the expansion of eq 9 and N_{basis} is the number of basis functions used to expand the wave function, evaluation of the similarity using a fitted density results in an N^2_{func}-dependent process, as opposed to an N^4_{basis}-dependent process when the exact density is used. It has been previously shown[24] that this methodology gives results with a mean deviation error smaller than 0.5% and with an important savings in computing time.

The fitting method used in this work was the so-called PSA method.[24] In this particular case, the set of $\{g_i\}$ functions has been chosen to be the same as the squared molecular s-type renormalized primitive functions. Linear dependency problems (such as those due to the presence of sp shells) have been avoided by using a set of independent functions. For

(19) Hammond, G. S. *J. Am. Chem. Soc.* **1955**, *77*, 334.

(20) Formosinho, S. J. In *Theoretical and Computational Models for Organic Chemistry*; Formosinho, S. J., Csizmadia, I. G., Arnaut, L. G., Eds.; Kluwer Academic Publishers: Dordrecht, 1991; p 159.

(21) Arteca, G. A.; Mezey, P. G. *J. Comput. Chem.* **1988**, *9*, 728.

(22) Duran, M.; Bertrán, J. *Rep. Mol. Theory* **1990**, *1*, 57. Solà, M.; Lledós, A.; Duran, M.; Bertrán, J.; Abboud, J.-L. M. *J. Am. Chem. Soc.* **1991**, *113*, 2873. Solà, M.; Carbonell, E.; Lledós, A.; Duran, M.; Bertrán, J. *J. Mol. Struct. (Theochem)* **1992**, *255*, 283.

(23) Varandas, A. J. C.; Formosinho, S. J. *J. Chem. Soc., Faraday Trans. 2* **1986**, *82*, 953. Formosinho, S. J. *J. Chem. Soc., Perkin Trans. 2* **1988**, *2*, 839. Parr, C.; Johnston, H. S. *J. Am. Chem. Soc.* **1963**, *85*, 2544. Agmon, N.; Levine, R. D. *Isr. J. Chem.* **1980**, *19*, 30. Agmon, N. *Int. J. Chem. Kinet.* **1981**, *45*, 343. Agmon, N.; Levine, R. D. *Chem. Phys. Lett.* **1977**, *52*, 197. Lendway, G. *J. Phys. Chem.* **1989**, *93*, 4422. Miller, A. R. *J. Am. Chem. Soc.* **1978**, *100*, 1984.

(24) Mestres, J.; Solà, M.; Duran, M.; Carbó, R. *J. Comput. Chem.*, in press.

(25) Mestres, J.; Solà, M.; Duran, M.; Carbó, R. In *Proceedings of the First Girona Seminar on Molecular Similarity*; Carbó, R., Ed., in press.

instance, if one uses the 6-31G*[26] basis set, each H atom contributes four Gaussian functions to the expansion of eq 9, whereas each C, O, or F adds 11 Gaussian functions to the expansion, and each S atom increases the number used in the expansion by 17. This results in a number of Gaussian functions in the expansion of eq 9 which is of the same order as the number of basis functions. Further, the $\Theta(r_1,r_2)$ operator in eq 7 has been taken as the Dirac delta function $\delta(r_1 - r_2)$ in the process of fitting the density. All the integrations are performed analytically over all space.

One of the main drawbacks of overlap-like QMSM is their important core dependence[25] due to the existence of cusps of electron density at nuclei. This fact means that once the mutual orientation of the two systems has been optimized, very small displacements of one system with respect to the other produce radical changes in the value of the overlap-like similarity. This problem can be circumvented through use of Coulomb-like QMSM, because the presence of the Coulomb operator smoothes the electron density surface. For this reason, throughout this paper the calculated QMSMs are Coulomb-like Similarities.

The recently defined NOEL similarity index[10] ($C_{A,B}$) shares several points with the widely used definition of QMSM given by eq 1.[14,15] In fact, the NOEL similarity index has been defined from the integral

$$\int\int [D_A(r_1,r_2) - D_B(r_1,r_2)]^2 \, dr_1 \, dr_2 \qquad (10)$$

by expanding the density matrices in terms of the natural spin orbitals

$$D_A(r_1,r_2) = \sum_i n_{Ai} \phi^*_{Ai}(r_1) \phi_{Ai}(r_2) \qquad (11)$$

and taking only the cross terms

$$C_{A,B} = \sum_{ij} n_{Ai} n_{Bj} |\langle \phi_{Ai} | \phi_{Bj} \rangle|^2 \qquad (12)$$

Equation 12 can also be obtained from eq 2 by setting $\Theta(r_1,r_2)$ to 1, *i.e.*, the NOEL method can also be seen as an overlap similarity between two first-order density matrices.

Using this definition, the NOEL similarity index has a clear physical interpretation, because it is equal to the number of electrons in the molecular fragments common to A and B. Another benefit of the NOEL index with respect to the definition of QMSM given by eq 1 is that it scales with the third power of the size of a molecular system. As expected, the value of the NOEL similarity index between two molecules increases with the number of electrons in the common fragments shared by the chemical structures of molecules A and B. However, most of the electronic contribution from the unshared fragments is lost due to the slight overlapping of their orbitals. For instance, the NOEL indices between molecules C_6H_6 and $C_6H_5NH_2$ or molecules C_6H_6 and $C_6H_5NO_2$ are almost the same,[10] not reflecting the clear density differences between the amine and nitro fragments. This notwithstanding, NOEL indices are especially suited to reflect similarities between molecules. On the other hand, eq 1 has been successfully applied to the calculation of QMSM for different chemical systems.[13,16,24,25] From these previous experiences, it can be concluded that QMSM as defined by eq 1 reflects both similarities and dissimilarities between molecules. The main disadvantage of this kind of QMSM turns out to be the high number of costly four-centered integrals. As shown before,[24,25] one can remove this drawback by using fitted densities, with practically no loss of accuracy, and the calculation then scales only as N^2_{func}.

The 6-31G*[26] basis set of Pople *et al.* has been used in all calculations except for the study of the Walden inversion reaction, where the 6-31+G[27] basis set has been preferred in order to describe adequately the electron density about negatively charged atoms. The SCF wave functions from which the electron density is fitted have been calculated by means of the Gaussian 90 system of programs.[28] When a uniform electric field has been taken into account, calculations of gradients and second derivative matrices have been performed with the Gaussian 90 package using nonstandard routes. The algorithm of Gonzalez and Schlegel[29a] was used for the computation of the intrinsic reaction path (IRP)[29b] with mass-weighted coordinates in order to get a physically meaningful reaction coordinate. The program used[30] in the computation of the QMSM allows one to optimize the mutual orientation of the two systems studied in order to maximize their similarity by the usual steepest-descent, Newton, and quasi-Newton algorithms.[31] This program is fully interfaced with the Gaussian 90[28] system of programs.

Table 1. Relative Energies (in kcal/mol) Referred to Reactants for the Different Species Involved in the F_2S_2/FSSF, HNC/HCN, H_2SO/HSOH, and H_2SCH_2/$HSCH_3$ Rearrangement Reactions Obtained with the 6-31G* Basis Set

	ΔE			
	F_2S_2/FSSF	HNC/HCN	H_2SO/HSOH	H_2SCH_2/$HSCH_3$
A	0.0	0.0	0.0	0.0
TS	72.5	39.8	53.8	8.0
B	−6.3	−12.5	−32.4	−95.2

Table 2. Similarity Measure (in au) Matrices between the Stationary Points for the F_2S_2/FSSF, HNC/HCN, H_2SO/HSOH, and H_2SCH_2/$HSCH_3$ Series of Reactions

	A	TS	B
		F_2S_2/FSSF	
A	1383.1828	1296.6973	1272.0407
TS		1374.2871	1258.4794
B			1365.2302
		HNC/HCN	
A	136.7545	136.1062	136.1717
TS		136.1059	135.8258
B			136.4243
		H_2SO/HSOH	
A	550.6272	534.8410	537.3564
TS		542.8570	542.6224
B			544.2355
		H_2SCH_2/$HSCH_3$	
A	499.1693	483.7926	494.1091
TS		490.8007	482.0409
B			505.7591

Results and Discussion

In this section we present first the results obtained for a group of four gas-phase rearrangement reactions and second the effect of an external perturbation on a Walden inversion reaction.

(A) Study of the F_2S_2/FSSF, HNC/HCN, H_2SO/HSOH, and H_2SCH_2/$HSCH_3$ Gas-Phase Reactions. Simple chemical gas-phase rearrangement reactions have been chosen in order to show how QMSM can be used as an interpretative tool for chemical reactivity.

Table 1 gathers the relative energies of reactants (A), products (B) and transition states (TS) of these four well-studied rearrangement reactions (see ref 32 for F_2S_2/FSSF, ref 33 for HNC/HCN, ref 34 for H_2SO/HSOH, and refs 34 and 35 for H_2SCH_2/$HSCH_3$). In this table, reactants have been selected

(26) Hehre, W. J.; Ditchfield, R.; Pople, J. A. *J. Chem. Phys.* **1972**, *56*, 2257. Francl, M. M.; Pietro, W. J.; Hehre, W. J.; Binkley, J. S.; Gordon, M. S.; Frees, D. J.; Pople, J. A. *J. Chem. Phys.* **1982**, *77*, 3654. Hariharan, P. C.; Pople, J. A. *Theor. Chim. Acta* **1973**, *28*, 213.

(27) Clark, T.; Chandrasekhar, J.; Spitznagel, G. W.; Schleyer, P. v. R. *J. Comput. Chem.* **1983**, *4*, 294.

(28) Frisch, M. J.; Head-Gordon, M.; Trucks, G. W.; Foresman, J. B.; Schlegel, H. B.; Raghavachari, K.; Binkley, J. S.; Gonzalez, C.; Defrees, D. J.; Fox, D. J.; Whiteside, R. A.; Seeger, R.; Melius, C. F.; Baker, J.; Martin, R. L.; Kahn, L. R.; Stewart, J. J. P.; Topiol, S.; Pople, J. A. *GAUSSIAN 90*, Revision H; GAUSSIAN Inc.: Pittsburgh, PA, 1990.

(29) (a) Gonzalez, C.; Schlegel, H. B. *J. Chem. Phys.* **1988**, *90*, 2154. (b) Truhlar, D. G.; Gordon, M. S. *Science* **1990**, *249*, 491.

(30) Mestres, J.; Solà, M.; Duran, M.; Carbó, R. *MESSEM*, version 1.0; Girona CAT, 1993.

(31) Scales, L. E. *Introduction to Non-Linear Optimization*; Springer-Verlag: New York, 1985.

(32) Solouki, B.; Bock, H. *Inorg. Chem.* **1977**, *16*, 665. Bickelhaupt, R. M.; Solà, M.; Schleyer, P. v. R., to be published.

(33) Müller, K.; Brown, L. D. *Theor. Chim. Acta* **1979**, *53*, 75. Gray, S. K.; Miller, W. H.; Yamaguchi, Y.; Schaefer, H. F., III. *J. Chem. Phys.* **1980**, *73*, 2733. Garrett, B. C.; Redmon, M. J.; Steckler, R.; Truhlar, D. G.; Baldridge, K. K.; Bartol, D.; Schmidt, M. W.; Gordon, M. S. *J. Phys. Chem.* **1988**, *92*, 1476. Bentley, J. A.; Bowman, J. M.; Gazdy, B.; Lee, T. J.; Dateo, C. E. *Chem. Phys. Lett.* **1992**, *198*, 563. Fan, L. Y.; Ziegler, T. *J. Am. Chem. Soc.* **1992**, *114*, 10890. Bentley, J. A.; Huang, C. N.; Wyatt, R. E. *J. Chem. Phys.* **1993**, *98*, 5207.

(34) Solà, M.; Gonzalez, C.; Tonachini, G.; Schlegel, H. B. *Theor. Chim. Acta* **1990**, *77*, 281.

Table 3. Similarity Indices (I), Distances (d) (Both in au), and Structural Proximity (β) and Isosynchronicity (α) Parameters for the F_2S_2/FSSF, HNC/HCN, H_2SO/HSOH, and H_2SCH_2/$HSCH_3$ Series of Reactions

reaction	$I_{A,B}$	$I_{A,TS}$	$I_{B,TS}$	$d_{A,B}$	$d_{A,TS}$	$d_{B,TS}$	α	β
F_2S_2/FSSF	0.9257	0.9405	0.9188	14.2944	12.8092	14.9183	1.9397	−0.1476
HNC/HCN	0.9969	0.9976	0.9968	0.9140	0.8050	0.9373	1.9062	−0.1447
H_2SO/HSOH	0.9816	0.9783	0.9983	4.4889	4.8788	1.3593	1.3897	0.7840
H_2SCH_2/$HSCH_3$	0.9834	0.9774	0.9675	4.0878	4.7313	5.6990	2.5516	−0.2367

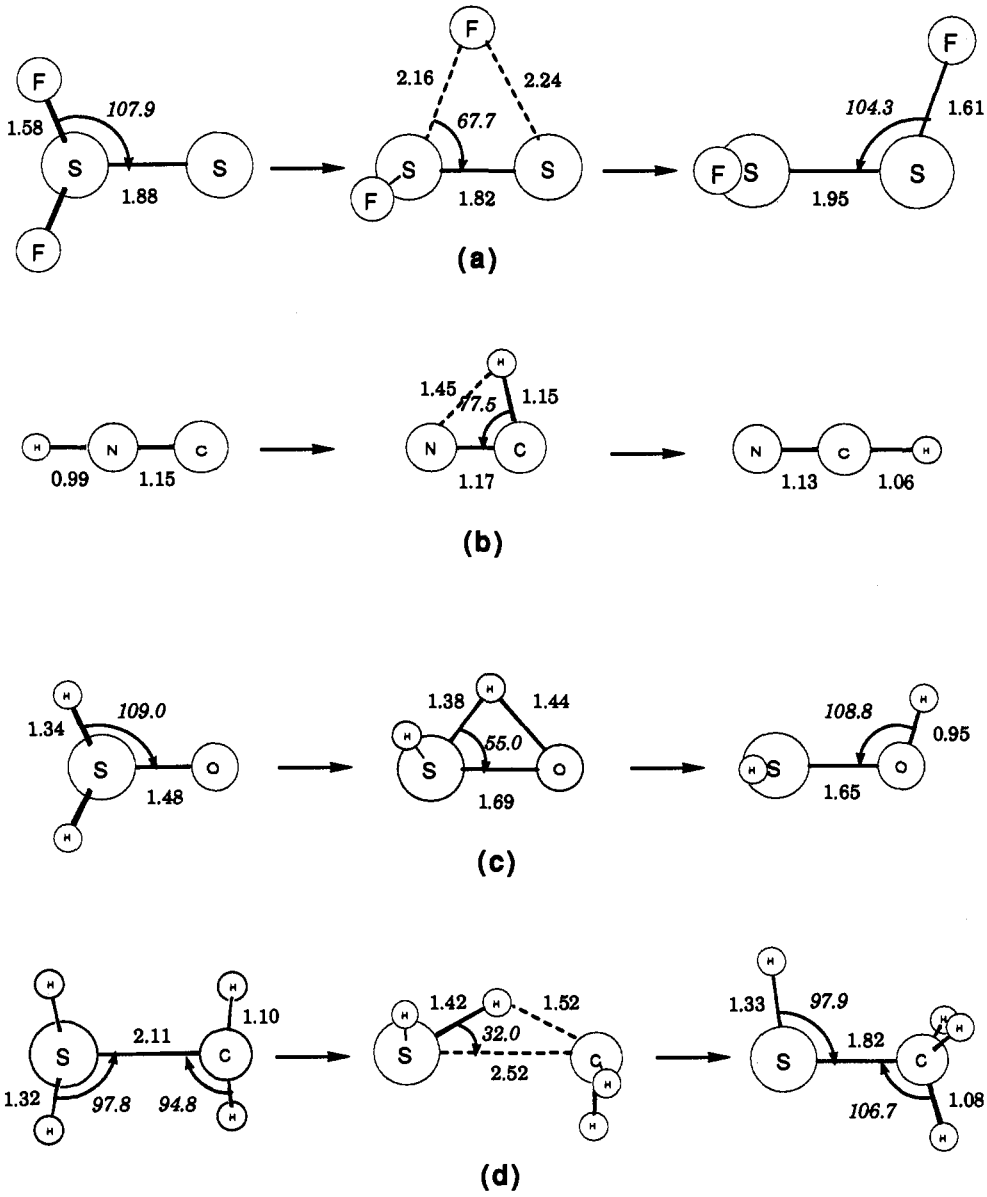

Figure 1. HF/6-31G* optimized geometries for the reactants, transition states, and products of F_2S_2/FSSF, HNC/HCN, H_2SO/HSOH, and H_2SCH_2/$HSCH_3$ rearrangement reactions. Bond lengths are given in angstroms and angles in degrees.

to be the nearest point in energy to the transition states. In Table 2, we collect the QMSM matrices for the four reactions studied. In Table 3, the I, distances, and α and β parameters as defined by Cioslowski obtained from the QMSM of Table 2 are given. Further, in Figure 1, the structures of reactants, transition states, and products together with the most significant geometrical parameters are depicted.

From the energy values of Table 1 and in the light of the Hammond postulate, it can be expected that the transition state of reaction F_2S_2/FSSF will be closer to F_2S_2 than to FSSF. Effectively, from the I and distances of Table 3 corresponding to this particular reaction, it can be seen that this result is properly reproduced: the distance of the TS to F_2S_2 (12.81 au) is shorter than that of the TS to the FSSF (14.92 au), thus giving rise to a negative value of β in this reaction, although its small absolute value (0.15) reflects the fact that the TS is found not far from the middle of the reaction coordinate. As can be seen in Table 3, there is a complete parallelism between I and the calculated distances: the higher the I is, the smaller the distance between the points becomes. This is not surprising, because cosine-like I and distances are well known to vary inversely with one to another.[14]

As regards the HNC/HCN rearrangement reaction, the most noticeable point is the small distances found between reactant,

(35) Mitchell, D. J.; Wolfe, S.; Schlegel, H. B. *Can. J. Chem.* **1981**, *59*, 3280. Eades, R. A.; Gassman, P. G.; Dixon, D. A. *J. Am. Chem. Soc.* **1981**, *103*, 1066. Dixon, D. A.; Dunning, T. H., Jr.; Eades, R. A.; Gassman, P. G. *J. Am. Chem. Soc.* **1983**, *105*, 7011.

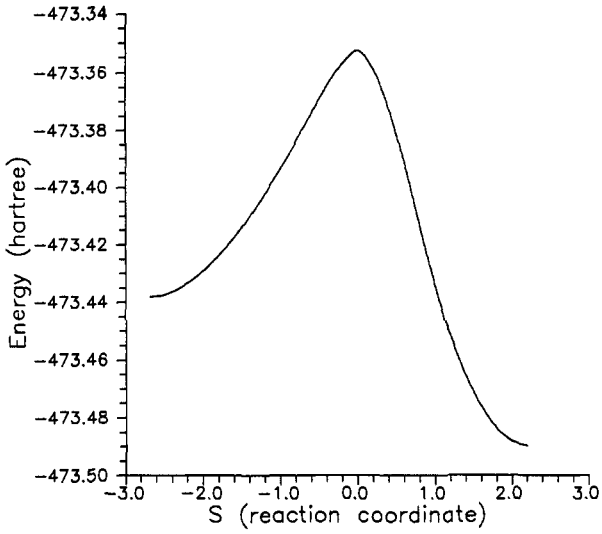

Figure 2. Potential energy profile of $H_2SO/HSOH$ rearrangement reaction computed with the 6-31G* basis set.

TS, and product. This can be easily interpreted from the geometric parameters corresponding to these complexes drawn in Figure 1b. In this reaction, the C–N bond length almost does not change when going from reactant to product, thus explaining the large values of the similarity indices and the small distances between stationary points. The small values of α and β reflect, respectively, the fact that in going from reactants to transition state small structural changes occur while the shape of the potential energy barrier remains almost symmetric.

Nevertheless, the most interesting rearrangement reaction turns out to be the $H_2SO/HSOH$ reaction. For this reaction, the IRP has been depicted in Figure 2. From this figure and from the values of the net reaction coordinate for reactants (–2.69) and products (2.19), it becomes apparent that this rearrangement reaction violates the predictions of the Hammond postulate. In this case, the TS is structurally closer to HSOH than to H_2SO, despite the fact that energetically this TS is closer to H_2SO than to HSOH. QMSM, as defined here, reproduce the anti-Hammond behavior, the distance between reactant and TS being larger (4.88) than the distance between product and TS (1.36) and also the similarity indices being smaller for reactant and TS than for product and TS. The positive value of β also shows that the TS is closer to product than to reactant. Finally, the small value of α due to the small distance between product and TS reflects the large, structurally speaking, similarity between product and TS. This can also be seen from the S–O bond length in Figure 1c: this value changes 0.21 Å when going from reactant to TS and only 0.04 Å from TS to product.

Anti-Hammond effects have been reported previously[36] for reactions in which change of a substituent leads to transition-state structures different from those predicted by the Hammond postulate and justified through changes of the transition state geometry perpendicular to the reaction coordinate. Also, these perpendicular effects have been attributed to a particular structure or configuration that contributes more to the TS than to reactants or products.[37] In this case, from Figure 2 it can be clearly seen that the force constants associated with reactants and products in the direction given by the transition vector are quite different, the force constant associated with products being larger than that associated with reactants and therefore accounting for the anti-Hammond behavior.

Table 4 compares the values of the net reaction coordinate and the distance from the TS obtained using eq 6 at selected points

(36) Jencks, W. P. *Chem. Rev.* **1985**, *85*, 511. Thornton, E. R. *J. Am. Chem. Soc.* **1967**, *89*, 2915. More O'Ferrall, R. A. *J. Chem. Soc. B* **1970**, 274. Bunnett, J. F. *Angew. Chem., Int. Ed. Engl.* **1962**, *74*, 731.

(37) Pross, A.; Shaik, S. S. *Acc. Chem. Res.* **1983**, *16*, 363.

Table 4. Net Reaction Coordinate and Distance (in au) to the Transition State (Computed with Eq 6) for Several Points Selected along the Mass-Weighted IRP for the $H_2SO/HSOH$ Rearrangement Reaction[a]

s	*d*	*s*	*d*
–2.69	4.88	0.00	0.00
–2.00	3.39	0.50	0.14
–1.50	2.06	1.00	0.38
–1.00	0.97	1.50	0.59
–0.50	0.32	2.19	1.36

[a] Negative values correspond to the reaction path giving rise to H_2SO.

of the mass-weighted IRP corresponding to the $H_2SO/HSOH$ rearrangement reaction. As one can see, the larger the net reaction coordinate, the larger the distance obtained. Although a direct quantitative relationship between the net reaction coordinate and the distance can not be inferred, these results validate the use of distances calculated from QMSM to predict the Hammond or anti-Hammond behavior, the latter becoming even more evident.

The $H_2SCH_2/HSCH_3$ rearrangement reaction is also found to follow Hammond behavior, the TS being closer to H_2SCH_2 than to $HSCH_3$. The distance between TS and H_2SCH_2 is found to be 4.73, whereas that between TS and $HSCH_3$ is 5.70. The negative value of β reflects again the Hammond behavior; the TS is more similar to the reactant than to the product. Interestingly, the large value of α is a consequence of the similarity between reactant and product being larger than either the similarity between TS and reactant or that between TS and product. This fact can be easily interpreted from Figure 1d, where one can see that for this reaction the S–C bond length changes from 2.113 Å in the reactant to 2.519 Å in the TS and to 1.818 Å in the product. Even in the case of Coulomb-like similarities, the value of the similarity depends strongly on the position and the overlap of the heaviest atoms (in this case, sulfurs and carbons). Therefore, the similarity between reactant and product is larger (and therefore the distance smaller) than that between either reactant or product and the TS. In this sense, it is interesting to regard this reaction as similar to the previous one, where the oxygen atom has been replaced by a CH_2 fragment, a less electronegative group. The effect of this substitution is of great importance since it changes completely the position of the TS along the reaction coordinate. This radical change can be explained by considering that in the $H_2SO/HSOH$ reaction, the H-rearrangement process is subject to the lengthening of the S–O bond (a 53.8 kcal/mol energy barrier needs to be surpassed): once the S–O bond length has been increased, the TS falls down easily to HSOH. However, in the $H_2SCH_2/HSCH_3$ reaction, the S–C bond is weak enough (only 8.0 kcal/mol from A to TS needs to be supplied) to permit the immediate H-rearrangement process, *i.e.*, the S–C bond length does not determine the reaction. Thus, as can be seen, the effect of different substituents on the potential energy profile can be studied in the QMSM context in order to predict and control the Hammond behavior.

As mentioned in the Introduction, small α values correspond to reactions with small distances from either A or B to the TS. This may suggest a possible relationship between the α values and the curvature of the IRP. In principle, a qualitative comparison between α and that curvature can be inferred: the larger the value of α, the smaller the curvature of the IRP at the TS. A further analysis shows us that different reaction paths with different curvatures but with identical energy differences between A, TS, and B may lead to the same α value. This means that the curvature of this kind of reaction path depends on the distance between reactants and products ($d_{A,B}$) and not only on the α values. Thus, a direct relationship between α and the IRP curvature cannot be established.

When comparing the values of β for the different reactions in Table 3, it can be seen that if in a given reaction one considers

Table 5. Geometrical Parameters (in Å) and Activation Energies (in kcal/mol) for the Walden Inversion Reaction When a Uniform Electric Field (F, in V/cm) Is Applied

F	$r_1 - r_2$	$r_1 + r_2$	E_{act}
	Reactant Complex (A)		
0.000	-1.1271	4.0875	12.13
5.140×10^6	-1.0744	4.0480	10.16
1.028×10^7	-1.0264	4.0136	8.34
2.056×10^7	-0.9369	3.9557	5.15
	Transition State (TS)		
0.000	0.0000	3.7766	
5.140×10^6	-0.0395	3.7767	
1.028×10^7	-0.0796	3.7768	
2.056×10^7	-0.1621	3.7779	
	Product Complex (B)		
0.000	1.1271	4.0875	12.13
5.140×10^6	1.1838	4.1332	14.26
1.028×10^7	1.2533	4.1897	16.55
2.056×10^7	1.4662	4.3780	21.74

B as the energetically more stabilized complex, then any reaction with a negative value of β follows the Hammond postulate, violating this postulate when positive values of β are found. It is also found that the larger the value of β is, the more asymmetric the energy profile becomes.

In conclusion, the previous results show that by taking advantage of the information provided by the QMSM, it is possible to draw an approximate shape of the computationally very demanding IRP, independent of the definition of the reaction coordinate being more or less complicated, allowing the prediction of the Hammond and anti-Hammond behaviour.

(B) Effect of External Perturbation on the Walden Inversion Reaction $F_a^- + H_3CF_b \rightarrow F_aCH_3 + F_b^-$. QMSM can also be used to perform a quantitative study of the change suffered by a given reaction under the effect of external perturbations. In particular, in this work the Walden inversion reaction $F_a^- + H_3CF_b \rightarrow F_a\text{-}CH_3 + F_b^-$ has been chosen to analyze, using QMSM, the effect of a uniform electric field applied along the F_a–C–F_b axis. The effect of this uniform electric field on the reaction path and on the potential energy profile of this process has been recently discussed.[38]

In Table 5, we have collected the geometrical and energetic parameters that completely characterize the process: r_1 and r_2 stand for the distances F_a–C and C–F_b, respectively; $r_1 - r_2$ usually taken as the reaction coordinate, reflects the internal change experienced by the process due to the transfer of the CH_3 group from F_a to F_b; $r_1 + r_2$ gives an idea of the change produced in the "skeleton" when the process advances; and finally, E_{act} is the activation energy when going from the reactant complex (A) or the product complex (B) to the transition state (TS).

From the activation energy values we can see that when the uniform electric field is applied, the reaction is catalyzed: the E_{act} for the reactant complex becomes smaller when the strength of the electric field applied increases. In addition, the electric field produces some changes in the structure of the stationary points. In particular, internal structural changes occur: comparing the $r_1 - r_2$ values for each stationary point when the field strength is increased, we can extract that while for A this value increases 0.1902 Å, for the TS this value diminishes 0.1621 Å. From these results we could say that A and TS are both getting internally closer. Further insight can be gained from the $r_1 + r_2$ values. It is interesting to observe that while A is compressed 0.1318 Å, the TS is only expanded 0.0013 Å, its "skeleton" remaining practically invariant. In fact, this structural rigidity

(38) Andrés, J. L.; Lledós, A.; Duran, M.; Bertrán, J. *Chem. Phys. Lett.* **1988**, *153*, 82. Carbonell, E.; Andrés, J. L.; Lledós, A.; Duran, M.; Bertrán, J. *J. Am. Chem. Soc.* **1988**, *110*, 996. Bertrán, J. In *New Theoretical Concepts for Understanding Organic Reactions*; Bertrán, J.; Cszimadia, I. G., Eds.; Kluwer Academic Publishers: Dordrecht, 1989; p 231. Mestres, J.; Duran, M. *Int. J. Quantum Chem.* **1993**, *47*, 307.

Table 6. Similarity Measure Matrices (in au) between the Stationary Points of the Walden Inversion Reaction (F in V/cm)

	A	TS	B
		$F = 0.000$	
A	380.2672	348.9983	358.0098
TS		384.5299	348.9983
B			380.2672
		$F = 5.140 \times 10^6$	
A	380.9682	352.8550	354.9702
TS		384.5313	344.9049
B			379.4648
		$F = 1.028 \times 10^7$	
A	381.5549	356.2651	347.3892
TS		384.5468	337.8963
B			378.5034
		$F = 2.056 \times 10^7$	
A	382.6267	363.2918	327.0365
TS		384.5885	325.2646
B			375.4293

of the TS in S_N2 reactions has been widely reported from both experimental and theoretical points of view.[39] Thus, from this point of view we could say that A is becoming more TS-like with the increase of the strength of the applied electric field.

In order to quantify how similar A or B are to TS, we have done several QMSM calculations. In Table 6, we have summarized the similarity measure matrices of the three stationary points for the different field strengths applied. The first noticeable result is that the self-QMSM of the TS remains practically invariant when the field strength is increased (it increases its value only 0.0586 when going from 0.0 to 2.056×10^7 V/cm). This value reflects the results obtained from the above analysis of the $r_1 + r_2$ values. Second, regarding the values of the self-QMSM of A for the different fields applied, we can observe that the similarity measure increases its value by 2.3595, getting closer to the value obtained for the self-QMSM of the TS. Finally, computing the distances as defined in eq 6 between reactants or TS at different electric fields, it is found that while the distance between A at 0.0 and A at 2.056×10^7 V/cm is 4.00, the distance between the TS at 0.0 and the TS at 2.056×10^7 V/cm is only 1.58, therefore indicating again that A undergoes larger electronic density changes than the TS does. Thus, from an electronic density point of view, it is A which evolves to TS when a uniform electric field is applied in order to catalyze the process. It is interesting to emphasize the fact that the relative magnitude of the self-QMSM of A, TS, and B reflects the dispersion of the electronic density in these different points: the more concentrated the electronic density is, the higher the self-QMSM becomes.

Once QMSM are known, one can obtain the similarity indices or distances to see how similar one point is to another and can calculate the transition-state parameters, α and β, previously defined by Cioslowski.[12] All these values have been collected in Table 7. An interesting result shows that for $F = 0.0$ and 5.140×10^6 V/cm, A is more similar to B than to the TS. This is due to the fact that in A and B the skeleton is substantially longer than that in the TS. When the field strength is increased, A becomes more similar to the TS, while B gets more dissimilar. Finally, referring to the α parameter, defined as the isosynchronicity parameter, it is worth noting that as A gets closer to the TS, α diminishes, and it is expected that when the strength of the electric field applied becomes strong enough to make the TS almost disappear,[38] α will reach the value of 1. On the other hand, with the increase of the electric field applied, the β parameter, defined as the structural parameter, becomes more negative, as one can expect from the Hammond postulate.

To sum up, it has been shown that a first approximation of the true reaction coordinate (taken as $r_1 - r_2$) indicates that the

(39) Shaik, S.; Schlegel, H. B.; Wolfe, S. *Theoretical Aspects of Physical Organic Chemistry. The S_N2 Mechanism*; Wiley: New York, 1992; pp 188–191 and references therein.

Table 7. Similarity Indices (I), Distances (d) (Both in au), and Structural Proximity (β) and Isosynchronicity (α) Parameters for the Walden Inversion Reaction When a Uniform Electric Field (F, in V/cm) Is Applied

F	$I_{A,B}$	$I_{A,TS}$	$I_{B,TS}$	$d_{A,B}$	$d_{A,TS}$	$d_{B,TS}$	α	β
0.000	0.9415	0.9127	0.9127	6.6719	8.1732	8.1732	2.4500	0.0000
5.140×10^6	0.9336	0.9219	0.9029	7.1058	7.7324	8.6131	2.3003	-0.1239
1.028×10^7	0.9141	0.9301	0.8857	8.0796	7.3193	9.3412	2.0620	-0.2502
2.056×10^7	0.8629	0.9470	0.8560	10.1972	6.3743	10.4637	1.6512	-0.4010

reactant A and the TS approach each other a similar amount upon increase of the electric field strength. In this kind of reaction, it is commonly concluded that the main effect of the electric field is to locate the TS earlier along the reaction coordinate, thus decreasing the energy barrier.[38] Nevertheless, considering the external "skeleton" ($r_1 + r_2$) of the process and the values of the QMSM along the reaction coordinate referred to the TS, it would be more exact to consider that it is the reactant complex which becomes more transition state-like and not that it is the transition state which acquires reactant-like character. Obviously, considering that it is the reactant that becomes transition state-like, the energy barrier is also reduced, thus explaining the observed results.

Conclusions

It has been shown that the quantum molecular similarity measures can be a useful interpretative tool for studying the relationships of proximity among minima and maxima of the potential energy surfaces. It has been demonstrated that the methodology presented in this work can be used to predict Hammond and anti-Hammond behavior at a lower CPU time cost than the expensive computation of the full mass-weighted intrinsic reaction coordinate for a given reaction. The changes of stable complexes and transition state on the potential energy surface due to the presence of external perturbations for a widely used model of the Walden inversion reaction have been clarified. It has been proved that, in this case, as the field strength increases, the reactant complex becomes more transition state-like, rather than, as usually stated, the transition state becoming more reactant-like.

Acknowledgment. This work has been funded through the DGICYT Project No. PB92-0333. J.M. acknowledges financial help provided by the Generalitat de Catalunya through CIRIT Project No. AR91-425. The authors are indebted to the referees for their fruitful comments.